PHOTONICS Research

Cnoidal waves and their soliton limits in single mode fiber lasers

Xiao Hu,[1,2] Tupei Chen,[2] Seongwoo Yoo,[2] and Dingyuan Tang[1,*]

[1]Julong College, Shenzhen Technology University, Shenzhen 518118, China
[2]School of Electrical and Electronic Engineering, Nanyang Technological University, Singapore 639798, Singapore
*Corresponding author: tangdingyuan@sztu.edu.cn

Received 12 October 2023; revised 10 January 2024; accepted 15 January 2024; posted 18 January 2024 (Doc. ID 508144); published 1 March 2024

Cnoidal waves are a type of nonlinear periodic wave solutions of the nonlinear dynamic equations. They are well known in fluid dynamics, but it is not the case in optics. In this paper we show both experimentally and numerically that cnoidal waves could be formed in a fiber laser either in the net normal or net anomalous cavity dispersion regime, especially because, as the pump power is increased, the formed cnoidal waves could eventually evolve into a train of bright (in the net anomalous cavity dispersion regime) or dark (in the net normal cavity dispersion regime) solitons. Numerical simulations of the laser operation based on the extended nonlinear Schrödinger equation (NLSE) have well reproduced the experimental observations. The result not only explains why solitons can still be formed in a fiber laser even without mode locking but also suggests a new effective way of automatic stable periodic pulse train generation in lasers with a nonlinear cavity.

https://doi.org/10.1364/PRJ.508144

1. INTRODUCTION

Periodic wave solutions have been found to exist in different nonlinear dynamic equations [1–11]. In solid state physics, such periodic nonlinear wave structures are known as Bloch waves that are reproduced self-consistently from crystal cell to cell. While the use of "Bloch waves" emphasizes the nature of lattice-periodically modulated plane waves in condensed matter, "cnoidal waves" are a more generally used nomenclature that connects the solutions to a large body of work on periodic wave structures in fluids, plasmas, and optics. Examples in optics include light propagation in micro-resonators and optical fibers. In the micro-resonator community, such periodic wave structures are also referred to as "turning rolls" that are governed by the Lugiato–Lefever equation (LLE) [12–14]. In optical fibers, such stationary periodic patterns are referred to as cnoidal waves that are described by the nonlinear Schrödinger equation (NLSE) [15]. In the NLSE approximation, while solitons are analytically expressed in terms of hyperbolic-secant [sech(x)] and tangent [tanh(x)] functions, cnoidal waves are expressed in terms of Jacobi elliptic functions [cn(x), sn(x), dn(x)] [16–19].

To date, the literature on cnoidal waves in fluids is extensive, but this is not the case in optics, except a few theoretical and/or numerical studies [20–22]. Among the various real physical systems, fiber lasers are routinely used as a platform for investigating complex nonlinear wave dynamics. Although a laser is intrinsically a dissipative system whose dynamics should be described by the extended Ginzburg–Landau equation (GLE), under steady state laser operation, the laser gain is always balanced by the cavity losses; furthermore, if the effect of gain bandwidth limitation could be neglected, the GLE is reduced to the NLSE [23]. Hence the light propagation in a fiber laser could mimic those of the NLSE dynamics, which justifies that under certain laser operation conditions NLSE solitons and cnoidal waves could be formed in a fiber laser. Both solitons and cnoidal waves of the NLSE are created by a balance between nonlinearity and dispersion. While soliton formation in fiber lasers has been experimentally extensively investigated, to the best of our knowledge, there has been no report on the experimental observation of cnoidal waves in a fiber laser. Physically, cnoidal waves bridge the gap between the CW and soliton states of a nonlinear system. In order to gain a comprehensive understanding on the dynamics of a fiber laser, it is important to study the properties and features of the cnoidal waves formed in it. In this work, we experimentally and numerically investigate the accessibility and stability of cnoidal waves in a single mode fiber laser either with net normal or net anomalous cavity dispersion. We show that compared to the formation of solitons, cnoidal waves, represented as a static periodic pulse train pattern in the laser cavity, can also be accessed in a fiber laser. It is interesting to note that stable periodic pulse patterns can also be frequently observed in mode-locked lasers through harmonic mode locking (HML) [24–28]. However, their formation mechanisms contrast starkly. In the scenario of HML, such periodic pulse trains are formed as a result of linear superposition of cavity modes. This is a process

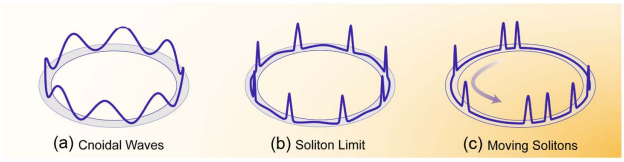

Fig. 1. Evolution of an NLSE cnoidal wave in a ring fiber cavity. Color gradient indicates the increase of cavity nonlinearity. (a) A cnoidal wave at low cavity nonlinearity. (b) A cnoidal wave at the soliton limit. (c) Particle-like freely running solitons.

that can be described by the conventional mode-locking theory, while the formation of cnoidal waves here could be viewed as a result of nonlinear light propagation in the fiber cavity. In this case the cavity modes are mutually coupled, and consequently the total optical field becomes synchronized with the cavity and behaves as a "super" nonlinear cavity mode, or in other words, becomes a periodic wave solution of the NLSE. A typical characteristic of the cnoidal waves is that in the limit of strong localization, the periodic pulses transform into bright/dark solitons. A similar feature is observed on the periodic waves formed in our fiber laser. Experimentally, as the pump power is increased, which corresponds to the increasing cavity nonlinearity, the periodic pulse trains evolve into periodic trains of solitons, corresponding to a frequency comb with increased power. The evolution of the state with the cavity nonlinearity could be illustrated as in Fig. 1. Different from the HML generated pulse patterns that always have typical narrow pulse widths, for instance, in the range of picoseconds in most cases, depending on the strength of the cavity nonlinearity, the periodic pulses in a cnoidal wave state could have pulse widths ranging from tens of nanoseconds to several picoseconds. A cnoidal wave state can be easily accessed in a fiber laser and could have any periodicity. This variability of the cnoidal wave states formed in a fiber laser is their great advantage compared to the traditional mode-locked pulses. Thus, the results not only provide a new approach to optically control the repetition rate and shape of nonlinear pulses but also assist in understanding the complexity in nonlinear science.

2. RESULTS

A. Experimental Setup

In our experiments, we perform time- and frequency-resolved measurements with a high-speed detection system consisting of a 40 GHz photodetector, a 33 GHz bandwidth real-time oscilloscope, and an optical spectrum analyzer. A schematic of the experimental setup is depicted in Fig. 2. All the fiber-pigtailed components (ISO, WDM, OC) used in the cavity are specially selected so that they have negligible polarization dependent loss and their functions are polarization independent; therefore, no conventional mode locking process could occur in our experimental setup. In this work, we prove that even without any mode-locking elements or external modulators, a simple fiber ring laser can still work as a flexible platform for the generation of a family of periodic nonlinear waves. Furthermore, by virtue of a careful management of the cavity nonlinearity and dispersion, we could investigate the formation

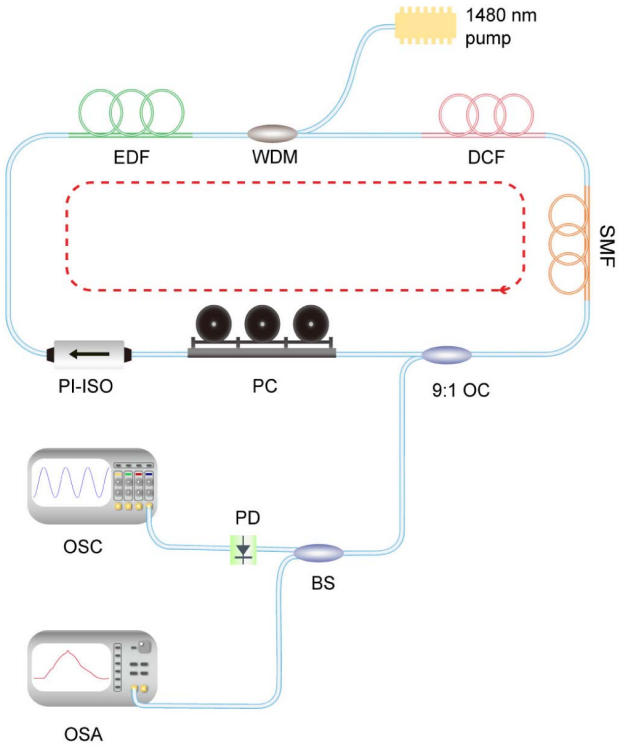

Fig. 2. Schematic of the experimental setup. The pump source is a 1480 nm Raman fiber laser. It has a maximum output power of 5 W. EDF, erbium-doped fiber (OFS-EDF80) with a group velocity dispersion (GVD) coefficient of $\beta_2 = 61.87$ ps^2/km; DCF, dispersion compensation fiber with a group velocity dispersion coefficient of $\beta_2 = 5.1$ ps^2/km; SMF, single mode fiber (SMF-28) with a group velocity dispersion coefficient of $\beta_2 = -21.94$ ps^2/km; PI-ISO, polarization independent isolator; WDM, wavelength division multiplexer; OC, output coupler; BS, beam splitter; PD, photodetector; PC, polarization controller; OSC, oscilloscope; OSA, optical spectrum analyzer.

of cnoidal waves and their soliton limits in both the normal and anomalous cavity dispersion regimes.

B. Cnoidal Waves in Anomalous Cavity Dispersion Regime

For demonstrating the existence of cnoidal waves, we construct the fiber ring cavity with 3 m EDF, 12 m SMF, 0 m DCF; thus, the net averaged cavity dispersion is tuned in the anomalous GVD regime, i.e., $\beta_{2,\mathrm{ave}} = -6.1$ ps^2/km. We emphasize that except the polarization controller (PC), which is used to fine adjust the cavity conditions, such as cavity nonlinearity and cavity detuning, no other polarization selective components or any saturable absorbers exist in our fiber laser. As all the intracavity components are polarization independent, no nonlinear polarization rotation (NPR) mode locking could occur in the laser. It is worth having a brief explanation on the functions of the intracavity PC. Through fine tuning the orientations of the PC paddles the effective intracavity birefringence would be changed, and consequently not only the laser oscillation wavelength but also the intracavity light power could be changed. Experimentally, through appropriately setting the intracavity

PC, we could even achieve multi-wavelength oscillation of our fiber laser.

We first operate our laser in the relatively low nonlinearity regime by injecting a relatively low pump power of 20 dBm. In all our experiments, under weak nonlinearities, the laser always displays CW emission. As we slowly increase the pump power to 22 dBm, a kind of periodic wave pattern with a period of $T = 50$ ps is obtained as shown in Fig. 3(a1). Once it is formed, the periodic pattern remains static in the cavity as shown in Fig. 4. Figure 3(a2) is the corresponding spectrum of Fig. 3(a1). Starting from such a state, if we slowly vary the intracavity PC paddles, other periodic wave emission states could also be obtained, as shown in Fig. 3(b1) (periodic wave with a period $T = 33$ ps) and in Fig. 3(c) (periodic wave with a period $T = 4$ ns). Operating in the low nonlinearity regime, the optical spectrum of the laser has a narrow band (–3 dB bandwidth is measured as ∼4 nm), and no Kelly sidebands are observed as indicated in the spectra shown in Figs. 3(a2) and 3(b2). From a state as shown in Fig. 3(a1), if the pump intensity is further increased to 24 dBm, the periodic wave then evolves into a state as shown in Fig. 5. The pulse train is still static in the cavity and remains the same pulse repetition rate as before, as shown in Fig. 5(a) (state measured at $t = 0$ s) and Fig. 5(b) (state measured at $t = 120$ s). However, with the increase in intracavity power, each peak of the periodic waves is obviously narrowed, as shown in Fig. 5(c). We experimentally

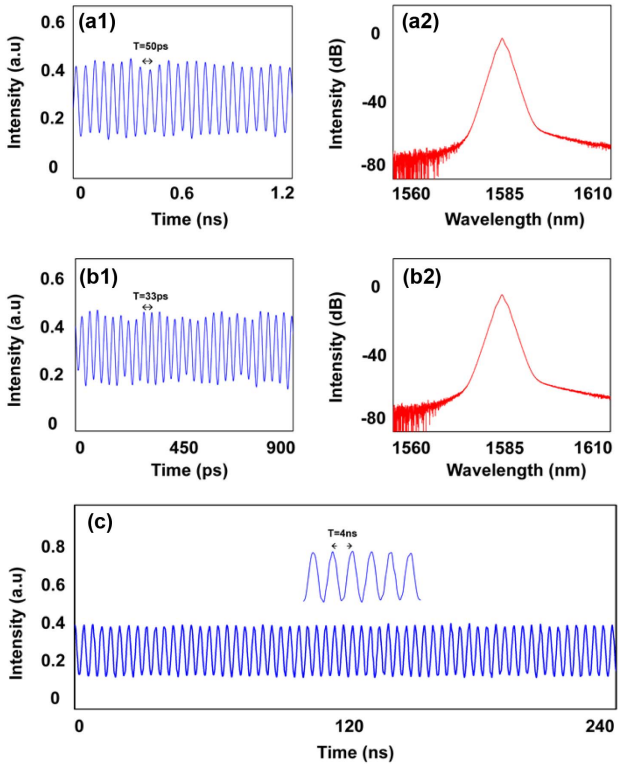

Fig. 3. Experimental results on formation of cnoidal waves with different periods in net anomalous dispersion regime. (a1) Oscilloscope trace of a cnoidal wave with period $T = 50$ ps. (a2) Corresponding optical spectrum for (a1). (b1) Oscilloscope trace of a cnoidal wave with period $T = 33$ ps. (b2) Corresponding optical spectrum for (b1). (c) Oscilloscope trace of a cnoidal wave with period $T = 4$ ns.

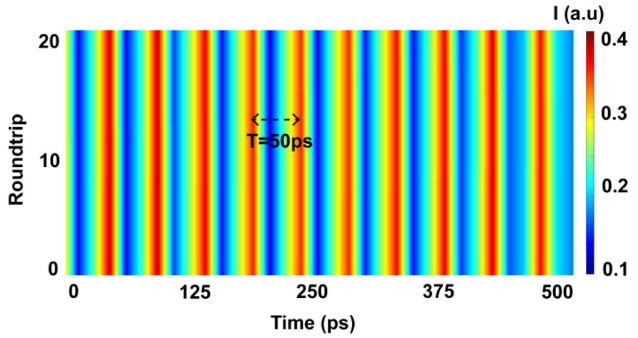

Fig. 4. Experimental results on evolution of the cnoidal wave with period $T = 50$ ps over 20 cavity roundtrips.

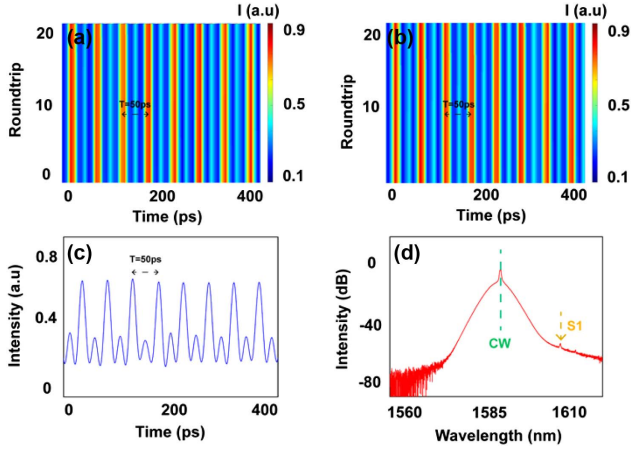

Fig. 5. Experimental results on soliton limit of cnoidal waves in net anomalous cavity dispersion regime. (a) Evolution of a periodic pulse train with period $T = 50$ ps measured at $t = 0$ s. (b) Evolution of the same periodic pulse train measured at $t = 120$ s. (c) A train of bright pulses with a typical pulse width around several picoseconds. (d) The corresponding optical spectrum of (c).

measured the autocorrelation trace of the pulses. It has a pulse width of 8 ps assuming a sech^2 pulse shape. Figure 5(d) shows the spectrum of the state. It is clearly broadened compared to that shown in Fig. 3(a2), meanwhile, a weak Kelly sideband, marked by the arrow S1, also appears on the spectrum. Kelly sidebands are formed as a result of interference between the solitons and dispersive waves in a laser, which is a unique characteristic of the soliton operation of a laser [29]. The appearance of such a weak Kelly sideband on the spectrum suggests that the obtained periodic pulses are approaching the soliton limit. We emphasize that despite the fact that the pulses already exhibit some of the soliton characteristics, i.e., broad spectral bandwidth and weak Kelly sidebands, they are not the NLSE type of particle-like solitons yet as they are static in the cavity. The experimentally observed evolution of the periodic pulses with the intracavity power (Fig. 4 to Fig. 5) is also verified by the numerical simulations shown in Figs. 6 and 7 (more details on the simulation model can be found in Ref. [23]). Figures 6(a)–6(f) show the formation of cnoidal

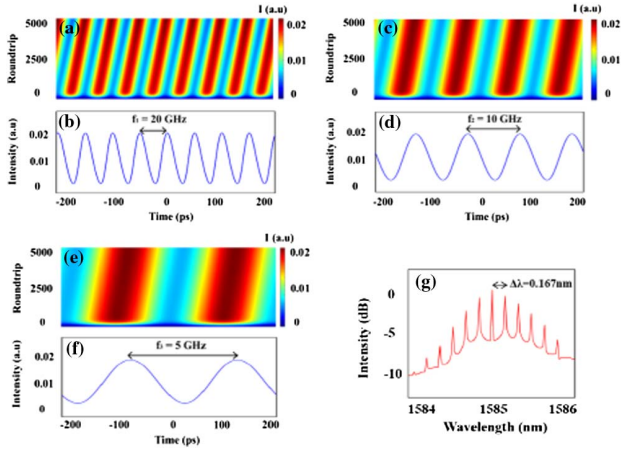

Fig. 6. Simulation results on formation of cnoidal waves with different period with net anomalous cavity dispersion. Parameters used in the simulation: A=0.01; $\beta_{2u,\mathrm{ave}} = -6.1$ ps^2/km; $g = g_0/[1 + \int(|u|^2 + |v|^2)\mathrm{d}t/E_s]$; $g_0 = 50$ km^{-1}; $E_s = 1$ pJ; $\gamma = 3$ W^{-1} km^{-1}. (a), (b) Stable formation of a cnoidal wave with period $T = 50$ ps; (c), (d) stable formation of a cnoidal wave with period $T = 100$ ps; (e), (f) stable formation of a cnoidal wave with period $T = 200$ ps. (g) Simulated optical spectrum for the cnoidal wave shown in (a).

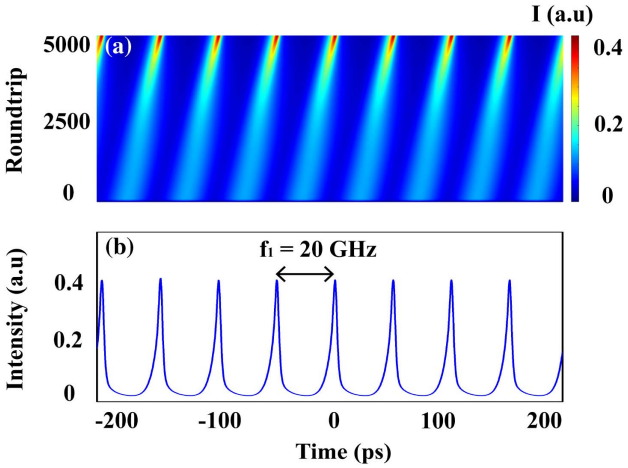

Fig. 7. Simulation result on a periodic bright pulse train formation. Except $g_0 = 80$ km^{-1}, the other parameters used are the same as those for Fig. 6(a).

waves with different periodicities (from 20 GHz to 5 GHz) in the net anomalous dispersion regime, and Fig. 6(g) is the optical spectrum for the case shown in Fig. 6(a). The spectrum shows obvious frequency comb, whose frequency separation matches well with the pulse repetition rate of the cnoidal wave. It is notable that limited by the resolution of our optical spectrum analyzer, only the envelope of the frequency comb could be visualized on the measured optical spectra of the cnoidal waves. Numerically we found that the cnoidal wave patterns could remain stable in the cavity even at weak nonlinearities, for instance, in all the three cases, the gain coefficient $g_0 = 50$ km^{-1}. Starting from a state as shown in Fig. 6(a), if we increase the intracavity power, the cnoidal wave pulses become narrower and narrower, and eventually at a gain coefficient $g_0 = 80$ km^{-1}, they evolve into a train of bright pulses. However, in all states the period of the pulses remains the same as shown in Fig. 7. The result is in good agreement with the experimental observations as shown in Figs. 4 and 5.

Experimentally, starting from a state as shown in Fig. 5, if we keep increasing the pump intensity to 27 dBm, the periodic pulses will finally evolve into the NLSE solitons, characterized by their obvious particle-like features; for instance, instead of remaining static, they start to move in the cavity as shown in Fig. 8(a) (soliton patterns measured at $t = 0$ s) and Fig. 8(b) (soliton patterns measured in the same time window but at $t = 120$ s). In addition, other signatures of a traditional NLSE soliton, e.g., the significant spectral broadening, and strong Kelly sidebands are also observed on the pulses as shown in Fig. 8(c). The solitons are randomly distributed in the cavity, meanwhile, undergoing collisions with each other. The exhibited features of the observed periodic waves are well in agreement with those of the cnoidal waves of the NLSE, as illustrated in Fig. 1. We emphasize that the above feature of the fiber laser is independent of the concrete cavity parameters such as cavity length, effective dispersion, and birefringence, and once the laser operation condition is appropriately set, it always occurs, suggesting that it is an intrinsic feature of the system.

We note that although periodic pulse trains could also be generated in a fiber through the modulation instability (MI) effect [30], the underlying formation mechanism and features of the formed pulse trains are starkly differed from those described above. Physically, modulation instability is essentially a four-wave mixing process where the Fermi-Pasta-Ulam (FPU) recurrence [31] always occurs. As a result, the pulse trains generated by the MI process exhibit pulse breather structures [32]. In addition, in a standard single mode fiber, determined by the fiber parameters, the modulation frequency of the

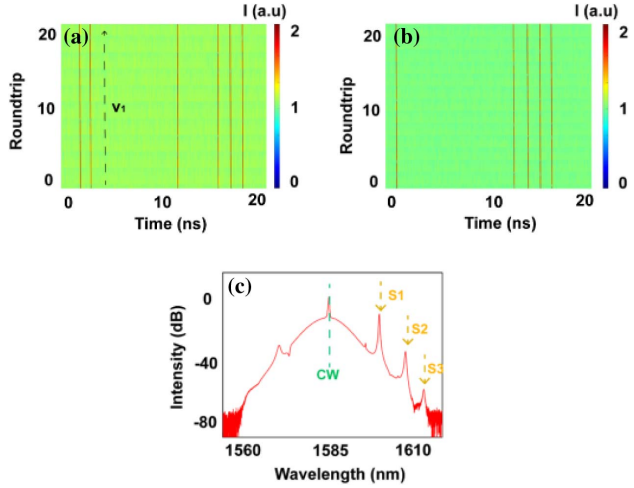

Fig. 8. Experimental results on a state with freely moving particle-like solitons. (a) Evolution of a soliton pattern measured at $t = 0$ s. (b) Evolution of a soliton pattern in the same time window but measured at $t = 120$ s. (c) The corresponding optical spectrum of (a).

MI is generally around hundreds of GHz, and the modulation frequency changes with the light intensity. Cnoidal waves are stationary eigenstate solutions of the nonlinear dynamic equations. In the framework of light propagation in single mode fibers, they can be interpreted as stationary periodic solutions of the cn and dn forms for the case of anomalous fiber dispersion and sn form for the case of normal fiber dispersion. The periodic pulse trains caused by the cnoidal waves exhibit no breather structures. In fact, MI is a general effect of nonlinear light propagation in anomalous dispersion fibers. Both theoretical and experimental studies have also shown that even the cn- and dn-types of cnoidal waves could become unstable due to occurrence of the MI [33].

Despite the fact that cnoidal waves are eigenstate solutions of the NLSE, in the practice it is difficult to generate automatically such a wave in a fiber transmission line. The situation is very different in the case of light propagation in a fiber ring laser. In a fiber laser the light is actually circulating in a cavity, where the cavity boundary condition should always be fulfilled [34,35], namely $E^{n+1}(Z=0,t)=\rho\exp(-i\phi)E^{n}(Z=L,t)$, where E is the complex envelope of the optical field, n denotes the nth passage through the cavity, and Z and t are the distance parameter and retarded time in a reference frame. L is the cavity length, and ρ and ϕ are the amplitude reflection and linear phase delay of the light generated after one roundtrip in the cavity. Previously it has been shown that light circulation in a detuned cavity could lead to the cavity-induced modulation instability (CIMI) [35,36], and such an MI effect has a much lower threshold than the conventional MI. CIMI could easily occur and destabilize the CW emission of a fiber laser, generating a weak periodic intensity modulation on the laser emission. As in the steady state laser operation, the optical field must be resonant with the laser cavity. Therefore, the cavity boundary condition naturally imposes a periodic condition on the laser oscillation, forcing the formation of cnoidal waves in a laser in the nonlinear regime. As the modulation frequency of CIMI varies with the cavity detuning, therefore, the formed cnoidal waves could have any periodicity, e.g., in our experiments, we have obtained stable periodic pulse trains with pulse repetition rate changed from hundreds of MHz to tens or even hundreds of GHz. As the observed periodic pulses are a cnoidal wave in nature, as we further increase the light intensity, the period of the pulse trains no longer changes. Increasing light intensity only modifies the energy localization parameter, and eventually, the pulses are shaped into their soliton limits (e.g., a train of soliton pulses with the same period as the cnoidal wave). The observed experimental results match well with the theoretical predictions in Refs. [16–19], suggesting that the experimentally obtained periodic pulse trains are indeed the cnoidal waves formed in the fiber laser. To the best of our knowledge, this is also the first clear experimental evidence on the cnoidal wave emission of a laser.

In most cases, a fiber laser could support multi-wavelength oscillations [37]. A typical optical spectrum of a dual-wavelength laser emission state is shown in Fig. 9, where similar to the case of Fig. 5(d), the central wavelength of a cnoidal wave (marked by blue dashed line in Fig. 9) is still centered at 1588 nm; in addition, through slightly varying the intracavity

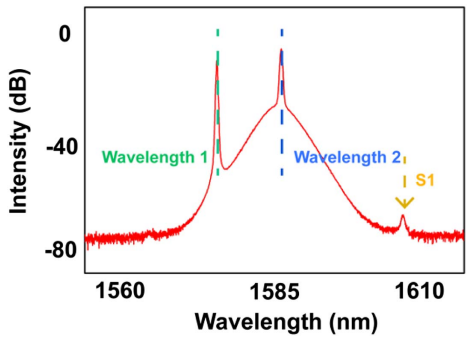

Fig. 9. Typical optical spectrum of dual-wavelength emission.

PC paddles, another laser oscillation with a central wavelength of 1575 nm (marked by green dashed line in Fig. 9) also appears. The two components coexist in the same cavity and interact with each other. As a result of their incoherent interaction, a kind of dual-wavelength domain structure is formed [38,39] as shown in Fig. 10(a), marked by the red solid line. We emphasize that the formation of the domains does not

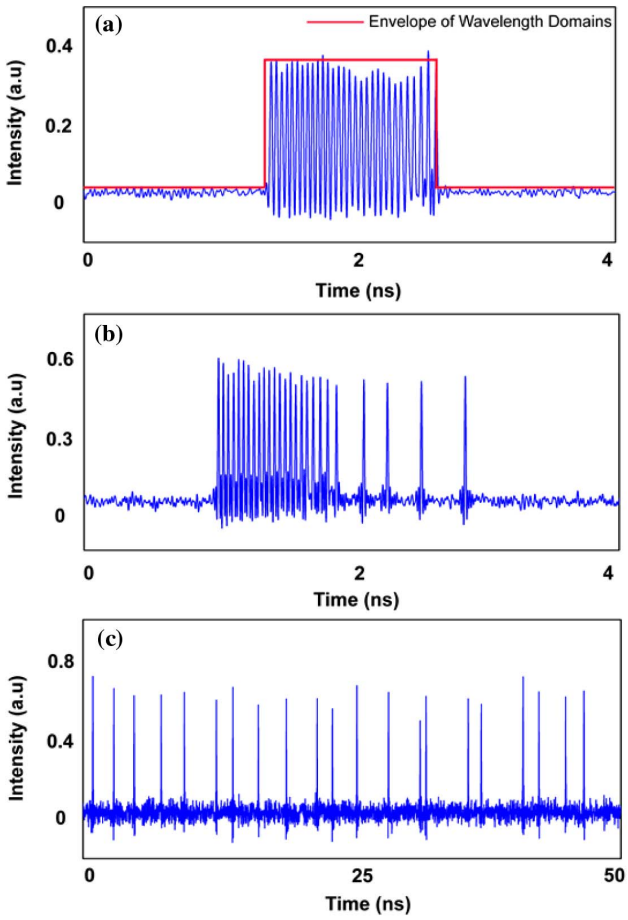

Fig. 10. Evolution of cnoidal waves in the case where the periodic boundary condition is redefined by the dual-wavelength domain walls. (a) Formation of a cnoidal wave within a wavelength domain. (b) Pulses on the right-hand side of the domain are shaped into solitons and run out of the domain. (c) Solitons fill up the whole laser cavity.

affect the formation of cnoidal waves, for instance, a periodic pulse train is still formed inside one domain region in the cavity, as shown in Fig. 10(a). Such a domain state was shown to be a solution of the cubic CGL equation [40,41]. Initially, the cnoidal wave is only formed in one domain, and the pulses are static in the domain. However, as we slowly increase the pump intensity from 22 dBm to 27 dBm, the pulses eventually start to run out of the domain, indicating that they are no longer bound to the other pulses but become a free NLSE soliton, as shown in Fig. 10(b). Finally, the solitons fill up the whole cavity as shown in Fig. 10(c). Note that the same process of cnoidal wave evolution is observed in the previous section (from Figs. 3–5). The only difference is that in previous cases, the periodic boundary is defined by the whole cavity length, but here it is redefined by the potential walls of the domains. The appearance of cnoidal waves in the domains could provide us with additional degrees of freedom to fine adjust the properties of the pulse trains, such as their duty-cycles. This could benefit their applications in fields of optical communication and ultrafast lasers.

In the NLSE approximation, not only the periodic cnoidal wave solutions could be supported; another special group of solutions, namely, "soliton on a cnoidal wave background" can also be supported [42]. We have also experimentally verified such a structure as shown in Fig. 11. In fact, the result of "soliton on a cnoidal wave background" could be interpreted as a case where a soliton and a cnoidal wave coexist in the system. Specifically, in the state shown in Fig. 11, bright solitons are formed on one of the laser oscillations whose central wavelength is λ_1, meanwhile, a cnoidal wave is formed on another laser oscillation whose central wavelength is λ_2. Because the effective laser gain at λ_1 is much larger than that at λ_2, solitons are formed at λ_1 due to the strong energy localization, while only the cnoidal wave is formed at λ_2. The formed solitons and cnoidal wave have different velocities as they have different central wavelengths, so it looks like that multiple bright solitons are riding on a noise background if the solitons are used as the oscilloscope trigger, as shown in Figs. 11(a) and 11(c). However, when we trigger the oscilloscope trace with the cnoidal wave background, its cnoidal wave feature becomes clear. It will show a periodic pulse pattern static in the cavity, as shown in Fig. 11(b), which matches well with the theoretical predictions in Ref. [42]. The inset of Fig. 11(c) shows a magnified view of the periodic cnoidal wave background, which has a period of around 63 ps. This result once again demonstrates that an appropriately designed fiber laser could be an ideal nonlinear testbed for the experimental studies of a large family of nonlinear wave solutions of the NLSE.

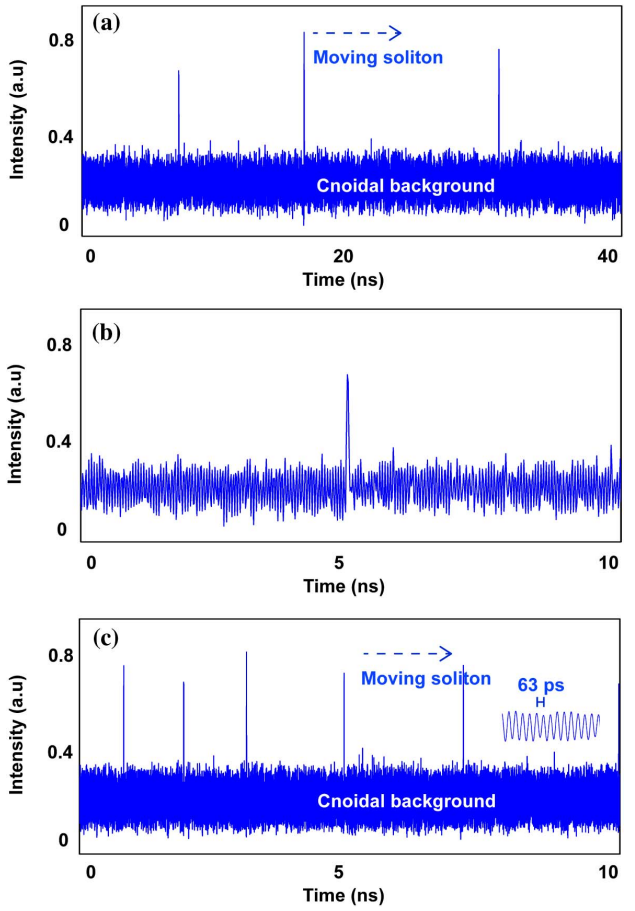

Fig. 11. Evolution of cnoidal waves in the case where the periodic boundary condition is redefined by the dual-wavelength domain walls. (a) Formation of a cnoidal wave within a wavelength domain. (b) Pulses on the right-hand side of the domain are shaped into solitons and run out of the domain. (c) Solitons fill up the whole laser cavity.

C. Cnoidal Waves in Net Normal Cavity Dispersion Regime

Experimentally, we also perform studies on cnoidal waves by operating the fiber laser at net normal cavity dispersion regime by selecting 3 m EDF, 5 m SMF, and 9 m DCF, and the averaged net cavity dispersion is therefore selected as $\beta_{2,\mathrm{ave}} = 6.58\ \mathrm{ps}^2/\mathrm{km}$. We first operate the laser in low nonlinearity regime by injecting a weak pump power of 23 dBm and obtain stable formation of cnoidal waves with two different periods, e.g., $T_1 = 2.5$ ns, $T_2 = 4$ ns as shown in Fig. 12(a) and Fig. 12(c), respectively. Figures 12(b) and 12(d) are the corresponding optical spectrum for Figs. 12(a) and 12(c), respectively. Two broad spectral sidebands are observable on the spectra (marked by arrows S1 and S2), and they were caused by the periodic power variation of the laser beam in the cavity [43]. They are not the Kelly sidebands.

Similar to the evolution of the cnoidal waves formed in the net anomalous dispersion regime, as we slowly increase the intracavity power by increasing the pump power from 23 dBm to 28 dBm, each pulse of the cnoidal waves as shown in Fig. 12(a) is narrowed; however, instead of transforming the pulses into a train of bright pulses, they are transformed into a train of dark pulses with typical pulse width around hundreds of picoseconds as shown in Fig. 13. Starting from such a soliton limit state, if we continue to increase the pump power to 30 dBm, the periodic dark pulses could finally be transformed into a train of black solitons with typical pulse width around several picoseconds. Nonetheless, it is important to note that the narrowest accessible pulse width is also limited by the net cavity dispersion; for instance, at large cavity dispersion, the narrowest pulse width obtainable is normally around hundreds of

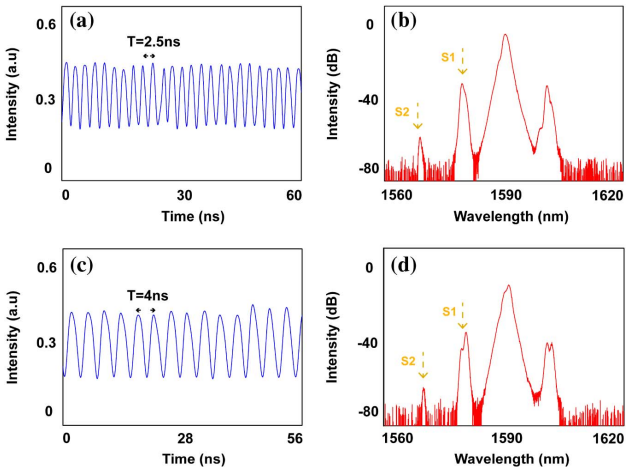

Fig. 12. Experimental results on formation of cnoidal waves with different periods in net normal dispersion regime. (a) Oscilloscope trace of a cnoidal wave with period $T = 2.5$ ns. (b) The corresponding optical spectrum of (a). (c) Oscilloscope trace of a cnoidal wave with period $T = 4$ ns. (d) The corresponding optical spectrum of (c).

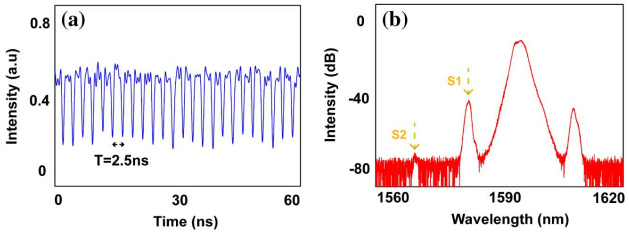

Fig. 13. Experimental results on the soliton limit of cnoidal waves in the net normal cavity dispersion regime. (a) A train of periodic dark pulses with a typical pulse width around hundreds of picoseconds. (b) The corresponding optical spectrum of (a).

picoseconds. In this scenario, further increasing pump intensity will result in dark pulse splitting instead of continuous narrowing of the pulse width [44].

To collaborate the experimental observations, we also numerically investigate the cnoidal wave formation and their soliton limit in the net normal cavity dispersion regime. Again, our simulations are based on our fiber laser cavity configuration of 3 m EDF, 5 m SMF, and 12 m DCF, thus an averaged net cavity dispersion of $\beta_{2u,\mathrm{ave}} = 6.1$ ps^2/km. It is interesting that in the normal dispersion regime, cnoidal wave structures can also be stably formed under weak cavity nonlinearity as shown in Fig. 14(a). Starting from a cnoidal wave state, as we increase the intracavity power by increasing the gain coefficient, the peaks of the cnoidal wave narrow down. To a gain coefficient $g_0 = 100$ km^{-1}, the cnoidal wave then evolves into a train of dark pulses, instead of bright pulses, as shown in Fig. 14(d). Figure 14(e) is the optical spectrum of the cnoidal wave state shown in Fig. 14(a). Again, the separation between the comb frequencies matches well with the repetition rate of the cnoidal wave pulses. This evolution of the cnoidal waves with the gain coefficient increase is again in good agreement with the experimental observations shown in Fig. 13. It is notable that

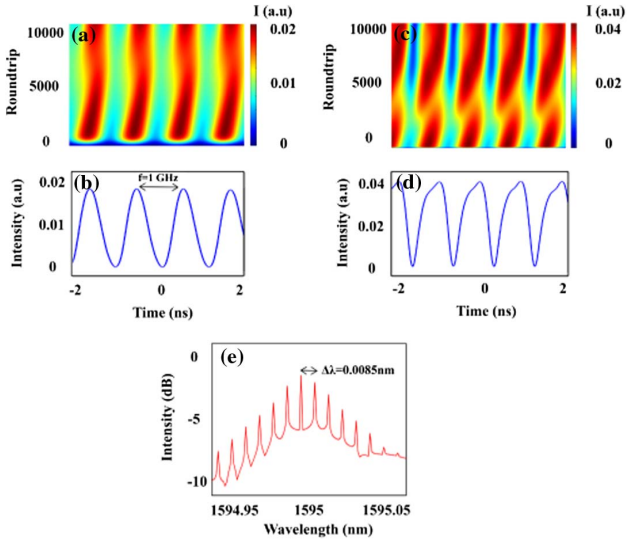

Fig. 14. Simulation results on the formation of cnoidal waves in the net normal cavity dispersion regime. Parameters used in the simulations: $A = 0.01; \beta_{2u,\mathrm{ave}} = 5.1$ ps^2/km; $g = g_0/[1 + \int(|u|^2 + |v|^2)\mathrm{d}t/E_s]; E_s = 1$ pJ; $\gamma = 3$ W^{-1} km^{-1}. (a) Evolution of a cnoidal wave with period $T = 1$ ns and $T = 1$ ns and $g_0 = 50$ km^{-1}. (b) A cnoidal wave pattern observed at the last cavity round trip of 10,000 in (a). (c) Evolution of a cnoidal wave to a train of dark pulses, $T = 1$ ns and $g_0 = 100$ km^{-1}. (d) Dark pulse pattern observed at the last cavity round trip of 10,000 in (c). (e) Simulated optical spectrum for the cnoidal wave state shown in (a).

experimentally either from the state shown in Fig. 5 or in Fig. 13, if the intracavity power is continuously increased, the cnoidal wave pulses would be transformed into the particle-like bright solitons (in anomalous fiber dispersion regime) or dark solitons (in anomalous fiber dispersion regime). Thereafter, they behave following the NLSE soliton theorem. Since the generation of ultrashort dark solitons is still a challenging task in many real-world physical systems, the presented method of dark soliton formation could be a superior alternative to the other method with the advantage of controllable dark pulse width in a wide range.

3. CONCLUSION

Obviously, independent of the sign of the net cavity dispersion, under suitable laser operation conditions, cnoidal waves can be easily formed in a fiber laser, and as the cavity nonlinearity increases, they could evolve into the soliton limit and even to the NLSE soliton regime. We note that although a cnoidal wave with strong energy localization could look very similar to an HML state frequently observed in a mode locked soliton fiber laser, they are two different states. A cnoidal wave state is a stationary periodic solution of the NLSE; in the state all the pulses in the cavity are mutually coupled, and therefore, they are static in the cavity or in the domains, while the solitons in an HML state are not mutually coupled. In agreement with the theoretical predictions, both cnoidal waves and solitons are stable solutions to the NLSE under different strength of nonlinearities. In our experiments, we have demonstrated an evolution route between the two states. This result also explains why periodic

pulse trains and NLSE solitons could still be obtained in a fiber laser, even without a saturable absorber or a mode-locker in the cavity. Thus, our finding provides a new approach for generating stable periodic optical pulse trains and optically controlling the periods and shapes of the optical pulses in a wide range. This technique could not only have impact on ultrafast lasers but also on other areas in which these features are crucial, such as broadband frequency combs [45], supercontinuum generation [46], and on-chip high-energy pulses for new applications in integrated photonics [47].

Although the NLSE can already reveal a large number of conservative periodic nonlinear wave varieties (including the presented cnoidal waves and their periodic soliton limits), in an attempt to investigate the light propagation in a femtosecond fiber laser, it is essential to start the exploration of nonlinear wave propagation with a higher order NLSE (HNLSE) that could support higher-order stationary periodic solutions such as "higher-order cnoidal waves." Compared with the case of conservative nonlinear structures supported by the standard NLSE, the impact of higher-order effects reveals unusual pulse profiles on such periodic wave structures, for instance, having a "pure square wave" or "bright soliton on top of square wave" pulse profile [48]. Finally, if the effective gain bandwidth limitation effect of a laser is no longer neglectable, the dissipative features of the system will play a dominant role. It is expected that even complicated periodic wave structures could be formed in the system. In view of the easy realization and stability of the formed nonlinear periodic waves in an active fiber cavity, it would be of both fundamental and practical importance to conduct comprehensive studies on features of the systems.

Funding. Natural Science Foundation of Top Talent of SZTU (GDRC202302); Department of Education of Guangdong Province (2022ZDJS116); Singapore Ministry of Education (RG114/21); Agency for Science, Technology and Research, Singapore (IRG M21K2c0109).

Acknowledgment. The research is sponsored in part by Department of Education of the Guangdong Province, Natural Science Foundation of Top Talent of SZTU.

Disclosures. The authors declare no competing interest.

Data Availability. Data underlying the results presented in this paper are not publicly available at this time but may be obtained from the authors upon request.

REFERENCES

1. P. St.J. Russell, T. A. Birks, and F. D. Lloyd-Lucas, "Photonic Bloch waves and photonic band gaps," in *Confined Electrons and Photons*, NATO ASI Series (1995), Vol. **340**, pp. 585–633.
2. V. N. Serkin, M. Matsumoto, and T. L. Belyaeva, "Bright and dark solitary nonlinear Bloch waves in dispersion managed fiber systems and soliton lasers," Opt. Commun. **196**, 159–171 (2001).
3. D. J. Korteweg and G. de Vries, "On the change of form of long waves in a rectangular canal, and on a new type of long stationary waves," Philos. Mag. **39**, 422–443 (1895).
4. G. B. Whitham, *Linear and Nonlinear Waves* (Wiley, 1974).
5. H. Schamel, "Analytical BGK modes and their modulational instability," J. Plasma Phys. **13**, 139–145 (1975).
6. A. E. Walstead, "A study of nonlinear waves described by the cubic nonlinear Schrödinger equation," Report UCRL-52920 (1980).
7. A. R. Osbourne, *Nonlinear Ocean Waves and the Inverse Scattering Transform* (Academic, 2010).
8. T. Kaladze and S. Mahmood, "Ion-acoustic cnoidal waves in plasmas with warm ions and kappa distributed electrons and positrons," Phys. Plasmas **21**, 032306 (2014).
9. G. P. Agrawal, *Nonlinear Fiber Optics* (Academic, 2001).
10. A. B. Matsko, A. A. Savchenko, W. Liang, *et al.*, "Mode-locked Kerr frequency combs," Opt. Lett. **36**, 2845–2847 (2011).
11. Y. K. Chembo and C. R. Menyuk, "Spatiotemporal Lugiato–Lefever formalism for Kerr-comb generation in whispering-gallery-mode resonators," Phys. Rev. A **87**, 053852 (2013).
12. Z. Qi, S. K. Wang, J. Jaramillo-Villegas, *et al.*, "Dissipative cnoidal waves (Turing rolls) and the soliton limit in microring resonators," Optica **6**, 1220–1232 (2019).
13. Z. Qi, G. D'Aguanno, and C. R. Menyuk, "Nonlinear frequency combs generated by cnoidal waves in microring resonators," J. Opt. Soc. Am. B **34**, 785–794 (2017).
14. Z. Qi, A. Leshem, J. A. Jaramillo-Villegas, *et al.*, "Deterministic access of broadband frequency combs in microresonators using cnoidal waves in the soliton crystal limit," Opt. Express **28**, 36304–36315 (2020).
15. V. Aleshkevich, Y. Kartashov, and V. Vysloukh, "Cnoidal waves compression by means of multisoliton effect," Opt. Commun. **185**, 305–314 (2000).
16. V. Aleshkevich and Y. Kartashov, "Self-frequency shift of cnoidal waves in a medium with delayed nonlinear response," J. Opt. Soc. Am. B **18**, 1127–1136 (2000).
17. Y. Kartashov, V. A. Vysloukh, E. M. Panameno, *et al.*, "Dispersion-managed cnoidal pulse trains," Phys. Rev. E **68**, 026613 (2003).
18. V. N. Serkin and A. Hasegawa, "Novel soliton solutions of the nonlinear Schrödinger equation model," Phys. Rev. Lett. **85**, 4502–4505 (2000).
19. L. H. Zhao and C. Q. Dai, "Self-similar cnoidal and solitary wave solutions of the (1+1)-dimensional generalized nonlinear Schrödinger equation," Eur. Phys. J. D **58**, 327–332 (2010).
20. Y. V. Kartashov, V. A. Vysloukh, and L. Torner, "Cnoidal wave patterns in quadratic nonlinear media," Phys. Rev. E **67**, 066612 (2003).
21. D. J. Kedziora, A. Ankiewicz, and N. Akhmediev, "Rogue waves and solitons on a cnoidal background," Eur. Phys. J. Spec. Top. **223**, 43–62 (2014).
22. K. Porsezian and B. Kalithasan, "Cnoidal and solitary wave solutions of the coupled higher order nonlinear Schrödinger equation in nonlinear optics," Chaos Solitons Fractals **31**, 188–196 (2007).
23. X. Hu, J. Guo, G. D. Shao, *et al.*, "Dissipative dark-bright vector solitons in fiber lasers," Phys. Rev. A **101**, 063807 (2020).
24. A. B. Grudinin and S. Gray, "Passive harmonic mode locking in soliton fiber lasers," J. Opt. Soc. Am. B **14**, 144–154 (1997).
25. C. M. Wu and N. K. Dutta, "High-repetition-rate optical pulse generation using a rational harmonic mode-locked fiber laser," IEEE J. Quantum Electron. **36**, 721–727 (2000).
26. J. Boguslawski, G. Sobon, R. Zybala, *et al.*, "Towards an optimum saturable absorber for the multi-gigahertz harmonic mode locking of fiber lasers," Photon. Res. **7**, 1094–1100 (2019).
27. F. Amrani, A. Haboucha, M. Salhi, *et al.*, "Passively mode-locked erbium-doped double-clad fiber laser operating at the 322nd harmonic," Opt. Lett. **34**, 2120–2122 (2009).
28. C. S. Jun, S. Y. Choi, F. Rotermund, *et al.*, "Toward higher-order passive harmonic mode-locking of a soliton fiber laser," Opt. Lett. **37**, 1862–1864 (2012).
29. S. M. J. Kelly, "Characteristic sideband instability of periodically amplified average soliton," Electron. Lett. **28**, 8–9 (1992).
30. K. Tai, A. Hasegawa, and A. Tomita, "Observation of modulational instability in optical fibers," Phys. Rev. Lett. **56**, 135–138 (1986).
31. B. Zhao, D. Y. Tang, and H. Y. Tam, "Experimental observation of FPU recurrence in a fiber ring laser," Opt. Express **11**, 3304–3309 (2003).
32. C. Y. Bao, J. A. J. Villegas, Y. Xuan, *et al.*, "Observation of Fermi-Pasta-Ulam recurrence induced by breather solitons in an optical microresonator," Phys. Rev. Lett. **117**, 163901 (2016).

33. G. Xu, A. Cabchoub, D. E. Pelinovsky, *et al.*, "Observation of modulation instability and rogue breathers on stationary periodic waves," Phys. Rev. Res. **2**, 033528 (2020).
34. D. Y. Tang, J. Guo, Y. F. Song, *et al.*, "Temporal cavity soliton formation in an anomalous dispersion cavity fiber laser," J. Opt. Soc. Am. B **31**, 3050–3056 (2014).
35. D. Y. Tang, J. Guo, Y. F. Song, *et al.*, "GHz pulse train generation in fiber lasers by cavity induced modulation instability," Opt. Fiber Technol. **20**, 610–614 (2014).
36. S. Coen and M. Haelterman, "Modulational instability induced by cavity boundary conditions in a normally dispersive optical fiber," Phys. Rev. Lett. **79**, 4139–4142 (1997).
37. D. Mao, H. Q. Wang, H. Z. Zhang, *et al.*, "Synchronized multi-wavelength soliton fiber laser via intracavity group delay modulation," Nat. Commun. **12**, 6712 (2021).
38. H. Zhang, D. Y. Tang, L. M. Zhao, *et al.*, "Dual-wavelength domain wall solitons in a fiber ring laser," Opt. Express **19**, 3525–3530 (2011).
39. Y. C. Meng, G. Semaan, M. Kemel, *et al.*, "Color domain in fiber lasers," Opt. Lett. **43**, 5054–5057 (2018).
40. B. A. Malomed, "Nonsteady waves in distributed dynamical systems," Physica D **8**, 353–359 (1983).
41. B. A. Malomed, "Evolution of nonsoliton and 'quasi-classical' wave trains in nonlinear Schrödinger and Korteweg-de Vries equations with dissipative perturbations," Physica D **29**, 155–172 (1987).
42. H. J. Shin, "Soliton on a cnoidal wave background in the coupled nonlinear Schrödinger equation," J. Phys. A **37**, 8017–8030 (2004).
43. X. Hu, J. Guo, J. Ma, *et al.*, "Periodic power variation induced sideband instability in a single mode fiber laser," Laser. Phys. Lett. **17**, 095103 (2020).
44. X. Hu, J. Guo, L. Li, *et al.*, "Evolution from periodic intensity modulations to dissipative vector solitons in a single-mode fiber laser," Photonics **7**, 103 (2020).
45. F. C. Meng, C. Lapre, C. Billet, *et al.*, "Intracavity incoherent supercontinuum dynamics and rogue waves in a broadband dissipative soliton laser," Nat. Commun. **12**, 5567 (2021).
46. A. V. Husakou and J. Herrmann, "Supercontinuum generation of higher order solitons by fission in photonic crystal fibers," Phys. Rev. Lett. **87**, 203901 (2001).
47. S. M. Hendrickson, A. C. Foster, R. M. Camacho, *et al.*, "Integrated nonlinear photonics: emerging applications and ongoing challenges," J. Opt. Soc. Am. B **31**, 3193–3203 (2014).
48. C. Q. Dai, Y. Y. Wang, and C. J. Yan, "Chirped and chirp-free self-similar cnoidal and solitary wave solutions of the cubic-quintic nonlinear Schrödinger equation with distributed coefficients," Opt. Commun. **283**, 1489–1494 (2010).